

# Testing No-Scale Supergravity with the Fermi Space Telescope LAT

Tianjun Li,<sup>1,2</sup> James A. Maxin,<sup>3</sup> Dimitri V. Nanopoulos,<sup>2,4,5</sup> and Joel W. Walker<sup>6</sup>

<sup>1</sup>*State Key Laboratory of Theoretical Physics and Kavli Institute for Theoretical Physics China (KITPC),  
Institute of Theoretical Physics, Chinese Academy of Sciences, Beijing 100190, P. R. China*

<sup>2</sup>*George P. and Cynthia W. Mitchell Institute for Fundamental Physics and Astronomy,  
Texas A&M University, College Station, TX 77843, USA*

<sup>3</sup>*Department of Physics and Astronomy, Ball State University, Muncie, IN 47306 USA*

<sup>4</sup>*Astroparticle Physics Group, Houston Advanced Research Center (HARC), Mitchell Campus, Woodlands, TX 77381, USA*

<sup>5</sup>*Academy of Athens, Division of Natural Sciences,  
28 Panepistimiou Avenue, Athens 10679, Greece*

<sup>6</sup>*Department of Physics, Sam Houston State University, Huntsville, TX 77341, USA*

We describe a methodology for testing No-Scale Supergravity by the LAT instrument onboard the Fermi Space Telescope via observation of gamma ray emissions from lightest supersymmetric (SUSY) neutralino annihilations. For our test vehicle we engage the framework of the supersymmetric grand unified model No-Scale Flipped  $SU(5)$  with extra vector-like flippon multiplets derived from F-Theory, known as  $\mathcal{F}$ - $SU(5)$ . We show that through compression of the light stau and light bino neutralino mass difference, where internal bremsstrahlung (IB) photons give a dominant contribution, the photon yield from annihilation of SUSY dark matter can be elevated to a number of events potentially observable by the Fermi-LAT in the coming years. Likewise, the increased yield in No-Scale  $\mathcal{F}$ - $SU(5)$  may also have rendered the existing observation of a 133 GeV monochromatic gamma ray line visible, if additional data should exclude systematic or statistical explanations. The question of intensity aside, No-Scale  $\mathcal{F}$ - $SU(5)$  can indeed provide a natural weakly interacting massive particle (WIMP) candidate with a mass in the correct range to yield  $\gamma\gamma$  and  $\gamma Z$  emission lines at  $m_\chi \sim 133$  GeV and  $m_\chi \sim 145$  GeV, respectively. Additionally, we elucidate the emerging empirical connection between recent Planck satellite data and No-Scale Supergravity cosmological models which mimic the Starobinsky model of inflation. Together, these experiments furnish rich alternate avenues for testing No-Scale  $\mathcal{F}$ - $SU(5)$ , and similarly structured models, the results of which may lend independent credence to observations made at the LHC.

PACS numbers: 11.10.Kk, 11.25.Mj, 11.25.-w, 12.60.Jv

## I. INTRODUCTION

Supersymmetry (SUSY) provides an elegant solution to naturally resolve the gauge hierarchy problem within the Standard Model (SM), and presuming  $R$  parity conservation, the lightest supersymmetric particle (LSP) neutralino serves as a viable cold dark matter (CDM) candidate [1, 2]. The empirical search for a weakly interacting massive particle (WIMP) currently evolves on multiple fronts. For instance, the Large Hadron Collider (LHC) at CERN sifts through trillions of proton-proton collisions for a rare glimpse of an anomalous missing transverse energy component of hypothetical supersymmetric interactions, where the SUSY LSP escapes the detector without direct observation as a consequence of its neutral  $U(1)_{EM}$  charge and status as an  $SU(3)_C$  singlet. Sharing an equivalent objective, the XENON [3], CDMS [4], and LUX [5] experiments parse through statistics gathered from ionization and scintillation of inert gases and semiconductors to potentially uncover direct observation of elastic collisions of a WIMP within the scintillating material. Likewise, the Fermi Space Telescope [6] strives toward this goal through latent observation of photon decay relics from WIMP annihilations. Status of observability for this latter conjectural phenomena, primarily within the context of a well defined model named No-Scale  $\mathcal{F}$ - $SU(5)$ , presides as the motivating in-

tent of this work; this approach offers a viable link between SUSY bino dark matter and a recently observed marginal sharp line spectra, and perhaps more pertinently, crafts a roadmap for future discovery of bino dark matter utilizing current and forthcoming sky-scanning surveys.

The annihilation of WIMPS within inner galactic regions can be prospective sources of gamma ray emissions that compete with the astrophysical background. SUSY LSP neutralinos can annihilate directly to gamma rays mono-energetically, yielding a (quasi-) monochromatic energy spectrum via annihilation processes  $\tilde{\chi}\tilde{\chi} \rightarrow \gamma\gamma$  ( $E_\gamma = m_\chi$ ),  $\tilde{\chi}\tilde{\chi} \rightarrow \gamma Z$ , and  $\tilde{\chi}\tilde{\chi} \rightarrow \gamma h$ . These processes occur at 1-loop, since WIMPS cannot directly couple to the photons, thereby suppressing the cross-section of thermally produced dark matter. Internal bremsstrahlung (IB) photons can also produce sharp spectral features with annihilation into charged particles via  $\tilde{\chi}\tilde{\chi} \rightarrow f\bar{f}\gamma$ , with the benefit that IB processes occur at tree level, thus providing a larger annihilation rate for bino neutralinos and amplifying observability.

In 2012, a tentative 130 GeV monochromatic gamma ray line was observed [7, 8] in the Fermi-LAT all sky surveys, exhibiting a local signal significance of  $4.3$ – $4.6\sigma$  ( $3.1$ – $3.3\sigma$  global). Post reprocessing of the data by the Fermi Collaboration, the budding signal shifted closer to 133 GeV with a diminished local signal significance of

$3.3\sigma$  (global  $1.6\sigma$ ) [9], somewhat dampening the enthusiasm for a prospective indirect discovery of dark matter. Additionally, a deviation at this same  $E_\gamma \sim 133$  GeV has been observed by the LAT instrument in a control sample of gamma rays from the Earth’s limb, elevating the likelihood that the reported effects are systematic in origin. Therefore, the jury remains out on the validity of the signal, and a conclusive judgment may not be pronounced for as much as two additional years, pending additional data acquisition and analysis. Yet, this tentative observation highlights the importance of a model dependent analysis of the Fermi-LAT’s reach into the supersymmetric parameter space. Due to the small bino annihilation cross-section of  $\langle\sigma v\rangle_{\gamma\gamma} \sim 10^{-30}$  cm<sup>3</sup>/sec, in comparison to the best fit of the deviation in the Fermi-LAT data of  $\langle\sigma v\rangle_{\gamma\gamma} \sim 10^{-27}$  cm<sup>3</sup>/sec [7, 8], the supersymmetric origins of the 130 GeV monochromatic gamma ray signal were quickly dismissed [10]. Minus the presence of an extraordinarily large boost factor ( $BF$ ) of  $BF \sim 1000$ , the cross-section of the observed 130 GeV signal seemed far too large for bino dark matter annihilations to two gamma rays to be a serious candidate.

Despite these objections to solicitation of a supersymmetric explanation for the 133 GeV gamma ray line, it was shown that a WIMP mass capable of producing  $\gamma\gamma$  emission at 133 GeV and  $\gamma Z$  emission at  $\sim 145$  GeV can be naturally explained [11] in the supersymmetric grand unified theory (GUT) model No-Scale flipped  $SU(5)$  with extra vector-like matter multiplets called “*flippons*” [11–34], the model referred to as  $\mathcal{F}\text{-}SU(5)$ . When considering a dominant contribution from the IB final states, the No-Scale  $\mathcal{F}\text{-}SU(5)$  upper  $2\sigma$  limit on the WIMP mass for the observed monochromatic gamma ray line is about  $M_{1/2} \sim 775\text{--}800$  GeV. While this particular SUSY mass is currently experiencing some tension from the LHC SUSY search [35], sufficient uncertainty remains in our spectrum calculations and Monte-Carlo simulations to likewise caution against its definitive exclusion until the 13 TeV LHC energizes in 2015.

Nonetheless, the more pressing question facing association of this result, or the prospect of a feasible near-term future Fermi-LAT observation at some heavier energy scale, with a genuine SUSY signal is that of whether an abnormally large boost factor is necessary to generate the observed photon flux. Moreover, this must be accomplished without overboosting fermion channels in the continuum; for instance, the stau-mediated channel with a  $\tilde{\chi}\tilde{\chi} \rightarrow \tau^+\tau^-$  final state, where the latest upper limit on the annihilation cross-section from observation of cosmic rays is  $\langle\sigma v\rangle_{\tau\tau} \lesssim 5 \times 10^{-25}$  cm<sup>3</sup>/sec [36], though parallel studies suggest the current limit could be as low as  $\langle\sigma v\rangle_{\tau\tau} \lesssim 3 \times 10^{-26} - 10^{-25}$  cm<sup>3</sup>/sec [37]. However, the SUSY mass  $M_{1/2} \sim 775$  GeV in No-Scale  $\mathcal{F}\text{-}SU(5)$  has an annihilation cross-section of  $\langle\sigma v\rangle_{\tau\tau} = 6.8 \times 10^{-29}$  cm<sup>3</sup>/sec, placing the necessarily required large boost factor of  $BF \sim 1000$  near the fringe of the upper limit allowed on any extraneous boost in the cross-section. It is thus preferable to pursue another course

that does not involve relying upon such a large boost factor. Because the IB photon flux is about an order or magnitude (to be concrete, around  $\sim 8 - 12\times$  [see Table II]) larger than the gamma gamma flux, the IB cross section is roughly 20 times larger than the gamma gamma cross section. Therefore, the No-Scale  $\mathcal{F}\text{-}SU(5)$  IB cross section is on the order of  $5 \times 10^{-29}$  cm<sup>3</sup>/sec. Thus, the corresponding boost factor that is needed to explain the 133 GeV Fermi-LAT gamma ray line in this scenario is substantively smaller, on the order of 50 to 100. If one allows that the dark matter density, which enters into the pairwise interaction as a square, is seven to ten times larger than what is traditionally used in the dark matter subhalo, this mechanism can explain the observed gamma ray line.

Regardless of whether the existing marginal 133 GeV gamma ray line eventually is shown to be a systematic or statistical effect, upcoming data from the Fermi Space Telescope (or future projects including Gamma-400, DAMPE and HERD) may provide exclusive insights into the SUSY parameter space in the No-Scale  $\mathcal{F}\text{-}SU(5)$  model. A central task confronted by this document is classification of the gamma ray signatures associable with  $\mathcal{F}\text{-}SU(5)$ , and quantification of their detection prospects across the model space, especially in the context of an additional six years of data collection by the Fermi-LAT instrument. Given the reality (failing upward revisions in estimates of the dark matter density profile) that the present generation gamma telescope will not achieve the sensitivity required to observe bino dark matter at annihilation cross-sections of  $\langle\sigma v\rangle_{\gamma\gamma} \sim 10^{-30}$  cm<sup>3</sup>/sec, we highlight a phenomenologically viable scenario where the probability of uncovering an observable indirect detection signature is somewhat more appreciable; in particular, we shall consider increasing the photon yield from annihilation via compression of the lightest slepton and LSP neutralino mass difference to near degeneracy, thereby establishing upward pressure on the annihilation rate, which can further elevate the advantage of the already dominant tree level IB effects over monochromatic loop level dark matter annihilation. This methodology can be quite naturally accommodated in No-Scale  $\mathcal{F}\text{-}SU(5)$  with no effect on the spectrum calculations and experimental constraints established in the model space [33]. The one unavoidable consequence of such a maneuver manifests itself in a suppressed bino neutralino relic density for  $M_{1/2} \lesssim 1500$  GeV, transitioning to below the recent Planck measurements [38], thereby compelling a non-thermal mechanism to generate the correct dark matter density. When the mass difference between the LSP neutralino and light stau is small, the LSP–light stau coannihilation cross section will be large, resulting in a dark matter relic density that is smaller than the observed value. Interestingly, cosmologically late decay of string-theoretic moduli fields provide an alternate mechanism for generating the correct dark matter relic density [39]. As the gaugino mass is increased from smaller values of  $M_{1/2}$  in No-Scale  $\mathcal{F}\text{-}SU(5)$ , a naturally occur-

ring linear compression in the light stau and LSP mass difference counteracts this bino relic density suppression in  $\mathcal{F}$ - $SU(5)$  [33] (*i.e.* elevation in the annihilation rate induced by mass degeneracy is counteracted by simple mass suppression), eventually generating the Planck measured CDM relic density  $\Omega h^2 = 0.1199 \pm 0.0027$  [38] at  $M_{1/2} \sim 1500$  GeV for a nearly degenerate light stau and LSP ( $\Delta M(\tilde{\chi}_1^0, \tilde{\tau}_1) \simeq 2$  GeV).

The No-Scale  $\mathcal{F}$ - $SU(5)$  framework suggested here as a vehicle for interpreting Fermi-LAT observations has already been well developed. The model is based upon the tripodal foundations of the dynamically established boundary conditions of No-Scale Supergravity, the Flipped  $SU(5)$  Grand Unified Theory (GUT), and the pair of TeV-scale hypothetical flippon vector-like supermultiplets [11–34] derived within local F-theory model building. The convergence of these features has been shown to naturally resolve many longstanding theoretical issues, whilst comparing positively with real world experimental observation. Moreover, a recent analysis [40–42] suggests that a cosmological model based upon the No-Scale supergravity sector yields compatibility with the Planck satellite measurements. With convenient superpotential parameter choices, the new cosmological model compatible with Planck data is a No-Scale supergravity realization of the Starobinsky model of inflation [43–45]. This prospective empirical evidence of the existence of a ubiquitous No-Scale supergravity sector amplifies our motivation for implementing No-Scale  $\mathcal{F}$ - $SU(5)$  as a realistic framework appropriate for evaluation against formerly recorded and forthcoming Fermi-LAT gamma ray emission statistics.

The structure of this paper is as follows. First we provide a brief review of the No-Scale  $\mathcal{F}$ - $SU(5)$  model, and then elaborate the interesting empirical correlation between recent Planck satellite data and cosmological models based upon No-Scale Supergravity that realize inflation in the Starobinsky mode. Next we shall present more detailed aspects of the IB effects on the annihilation rate and, finally, we present some benchmark models with SUSY spectra linked to neutralino annihilation cross-sections testable by the Fermi Space Telescope in the upcoming years, as well as benchmarks consistent with a No-Scale  $\mathcal{F}$ - $SU(5)$  explanation of the observed 133 GeV monochromatic gamma ray line.

## II. THE NO-SCALE $\mathcal{F}$ - $SU(5)$ MODEL

Mass degeneracy of the superpartners has not been observed, indicating that SUSY breaking occurs near the TEV scale. Supergravity models are GUTs with gravity mediated supersymmetry breaking, where we can fully characterize the supersymmetry breaking soft terms by a limited set of universal parameters: universal gaugino mass  $M_{1/2}$ , universal scalar mass  $M_0$ , Higgsino mixing  $\mu$ -parameter, Higgs bilinear  $B_\mu$ -parameter, and universal trilinear coupling  $A_0$ . The  $B_\mu$  and  $|\mu|$  parameters are

then determined at low energy through minimization of the Higgs potential triggering radiative electroweak symmetry breaking (REWSB), with the sign of  $\mu$  remaining undetermined. Equivalently, we can trade  $B_\mu$  at low energy for the low energy ratio of the Higgs vacuum expectation values (VEVs)  $\tan\beta$ . Subsequently remaining are the high-energy boundary conditions  $M_{1/2}$ ,  $M_0$ ,  $B_\mu$ ,  $A_0$ , and the low energy boundary condition  $\tan\beta$ , plus the undetermined sign of  $\mu$ , which we always take to be  $\text{sgn}(\mu) > 0$ , as suggested by the results of  $(g_\mu - 2)/2$  of the muon.

In order to address the cosmological flatness problem, No-Scale Supergravity was proposed [46] as the subspace of supergravity models which fulfill three constraints: i) the vacuum energy vanishes automatically due to the appropriate Kähler potential; ii) there exist flat directions that leave the gravitino mass  $M_{3/2}$  undetermined at the minimum of the scalar potential; iii) the quantity  $\text{Str}\mathcal{M}^2$  is zero at the minimum. Large one-loop corrections would force  $M_{3/2}$  to be either identically zero or of the Planck scale if the third condition were violated. A minimal Kähler potential that meets the first two conditions is [46, 47]

$$K = -3\ln(T + \bar{T} - \sum_i \bar{\Phi}_i \Phi_i), \quad (1)$$

where  $T$  is a modulus field and  $\Phi_i$  are matter fields, which parameterize the non-compact  $SU(N, 1)/SU(N) \times U(1)$  coset space. The third condition can always be satisfied in principle and is model dependent [48]. From the Kähler potential in Eq. (1) we automatically attain the No-Scale boundary condition  $M_0 = A_0 = B_\mu = 0$ , while  $M_{1/2}$  is allowed to be non-zero and hence evolve naturally, and in fact, is necessary for SUSY breaking. Moreover, the high-energy boundary condition  $B_\mu = 0$  in principle determines  $\tan\beta$  at low energy. The gravitino mass  $M_{3/2}$  is determined by the equation  $d(V_{EW})_{\min}/dM_{3/2} = 0$  due to the fact that the minimum of the electroweak (EW) Higgs potential  $(V_{EW})_{\min}$  depends on  $M_{3/2}$ , and consequently, the supersymmetry breaking scale is determined dynamically. We are thus left with a natural *one-parameter* model, with the sole degree of freedom being the gaugino mass  $M_{1/2}$ . As a deep fundamental correlation to string theory, No-scale supergravity can be realized in the compactification of the weakly coupled heterotic string theory [49], as well as the compactification of M-theory on  $S^1/Z_2$  at the leading order [50].

Precise string-scale gauge coupling unification while also evading the Landau pole problem can be realized by supplementing the standard  $\mathcal{F}$ -flipped  $SU(5) \times U(1)_X$  [51–54] SUSY field content with the following TeV-scale vector-like multiplets (flippons) [55]

$$\begin{aligned} (XF_{(10,1)} \equiv (XQ, XD^c, XN^c), \overline{XF}_{(\overline{10},-1)}) , \\ (Xl_{(1,-5)}, \overline{Xl}_{(1,5)} \equiv XE^c) , \end{aligned} \quad (2)$$

where  $XQ$ ,  $XD^c$ ,  $XE^c$ ,  $XN^c$  have the same quantum numbers as the quark doublet, the right-handed

down-type quark, charged lepton, and neutrino, respectively. Models of this nature can be realized in  $\mathcal{F}$ -ree  $\mathcal{F}$ -fermionic string constructions [56] and  $\mathcal{F}$ -theory model building [57, 58], and have been appropriately designated  $\mathcal{F}$ - $SU(5)$  [57].

The split-unification framework of  $\mathcal{F}$ - $SU(5)$  [51–54] provides for fundamental GUT scale Higgs representations (not adjoints), natural doublet-triplet splitting, suppression of dimension-five proton decay [54, 59], and a two-step see-saw mechanism for neutrino masses [60, 61]. Adjustments to the one-loop gauge  $\beta$ -function coefficients  $b_i$  induced by inclusion of the vector-like flippon multiplets generate the required flattening of the  $SU(3)$  Renormalization Group Equation (RGE) running ( $b_3 = 0$ ) [12], which manifests as a wide separation between the primary  $SU(3)_C \times SU(2)_L$  unification near  $10^{16}$  GeV and the secondary  $SU(5) \times U(1)_X$  unification near the Planck mass. The corresponding baseline extension for logarithmic running of the No-Scale boundary conditions, especially that of  $B_\mu = 0$ , permits ample scale for natural dynamic evolution into phenomenologically favorable values consistent with experiment at the EW scale. The  $SU(3)_C$  gaugino mass scale flattening generates a stable characteristic mass texture of  $M(\tilde{t}_1) < M(\tilde{g}) < M(\tilde{q})$ , engendering a light stop and gluino that are lighter than all other squarks [12].

The No-Scale  $\mathcal{F}$ - $SU(5)$  model space satisfies a minimal set of necessary constraints from theory and phenomenology [18, 33]. The constraints are: i) consistency with the dynamically established boundary conditions of No-Scale supergravity (most significantly the strict enforcement of a vanishing  $B_\mu$  parameter at the ultimate flipped  $SU(5)$  GUT unification near  $M_{\text{Pl}}$ , imposed as  $|B_\mu(M_{\mathcal{F}})| \leq 1$  GeV, about the scale of the EW radiative corrections); ii) REWSB; iii) the centrally observed Planck CDM relic density  $\Omega h^2 = 0.1199 \pm 0.0027$  [38]; iv) the world average top-quark mass  $m_t = 173.3 \pm 1.1$  GeV [62]; v) precision LEP constraints on the light SUSY chargino and neutralino mass content [63]; and vi) production of a lightest CP-even Higgs boson mass of  $m_h = 125.5 \pm 1.5$  GeV, accomplished through additional tree level and one-loop contributions to the Higgs boson mass by the flippon supermultiplets [11, 25, 33], supplementing the Minimal Supersymmetric Standard Model (MSSM) Higgs boson mass by just the essential additional 3-5 GeV amount requisite to attain  $m_h \sim 125$  GeV, while also preserving a testably light SUSY spectrum that does not reintroduce the gauge hierarchy problem via very heavy scalars that SUSY was originally intended to solve in the first place. A two-dimensional parameterization in the vector-like flippon super-multiplet mass scale  $M_V$  and the universal gaugino boundary mass scale  $M_{1/2}$  is excised from a larger four-dimensional hyper-volume that also includes the top quark mass  $m_t$  and the ratio  $\tan\beta$ . The enduring model space after application of these minimal constraints is capable of maintaining the delicate balance needed to realize the two conditions  $B_\mu = 0$  and  $\Omega h^2 = 0.1199 \pm 0.0027$ .

The surviving No-Scale  $\mathcal{F}$ - $SU(5)$  model space after direct application of the constraints noted above consists of a diagonal wedge (*cf.* Ref. [33]) in the  $(M_{1/2}, M_V)$  space, the width of which at small  $M_{1/2}$  and small  $M_V$  is bounded by the LEP constraints and by the CDM constraints and the transition to a charged stau LSP at large  $M_{1/2}$  and large  $M_V$ . Conversely, the upper limit at large  $M_V$  and the lower limit at small  $M_V$  are constrained by the central experimental range on the top quark mass. The intersection of all constraints yields a net experimentally viable model space extending from  $M_{1/2} \simeq 400$  GeV to  $M_{1/2} \simeq 1500$  GeV, with an associated vector-like flippon mass of  $M_V \simeq 1$  TeV to  $M_V \simeq 180$  TeV.

### III. NO-SCALE SUPERGRAVITY INFLATION

The elegantly minimalistic formalism of No-Scale Supergravity [46, 47, 64–66] allows for a deep fundamental correlation to string theory in the infrared limit, the natural inclusion of general coordinate invariance (general relativity), a supersymmetry breaking mechanism that preserves a vanishing cosmological constant at tree level (facilitating the observed longevity and cosmological flatness of our Universe [46]), natural suppression of CP violation and flavor-changing neutral currents, dynamic stabilization of the compactified spacetime by minimization of the loop-corrected scalar potential, and a powerful contraction in parameterization freedom.

Recently, an added phenomenological boost has been given to No-Scale Supergravities by detailed measurement of the Cosmic Microwave Background (CMB) perturbations (the structural seeds of galactic supercluster formation residually imprinted upon the faint afterglow of the big bang) from the Planck [67] satellite. Many important features predicted qualitatively by the cosmological inflationary paradigm have been borne out, for instance, there are no significant signs of non-Gaussian fluctuations or hints of non-trivial topological features such as cosmic strings. Additionally, these observations verified a highly statistically significant tilt  $n_s \simeq 0.960 \pm 0.007$  in the spectrum of scalar perturbations, as expected if the effective scalar energy density decreased gradually during inflation, and set stronger upper limits on the ratio  $r < 0.08$  of tensor (directional) to scalar (isotropic) perturbations. These measurements, particularly of  $n_s$ , place many leading models of cosmic inflation in jeopardy (*cf.* Fig. 1 of Ref. [67]), although a curious scenario suggested by Starobinsky [43] in 1980 is known [44] to match the data effortlessly. This model is a rather ad-hoc modification of Einstein's description of gravity, which combines a quadratic power of the Ricci scalar with the standard linear term. At face value, this  $(R + R^2)$  model is rather difficult to take seriously, but there is substantial enthusiasm for the observation by John Ellis, Keith Olive and one of the authors (D.V.N), that this esoteric model is in fact conformally equivalent to No-Scale supergravity with an  $SU(2,1)/SU(2) \times U(1)$

Kähler potential [40–42], which is a subcase of Eq. (1). To be specific, the algebraic equations of motion corresponding to an auxiliary scalar field  $\Phi$  with a quadratic potential that couples to a conventional Einstein term may be freely substituted back into the action, resulting in the phenomenologically favorable quadratic power of the scalar curvature [68, 69]. In short, inflation in our  $\mathcal{F}$ - $SU(5)$  No-Scale  $SU(N, 1)$  framework can be realized naturally and is consistent with the Planck results.

#### IV. TESTING NO-SCALE $\mathcal{F}$ - $SU(5)$ WITH FERMILAT

The monochromatic line signals are not the only mechanism capable of generating gammas visible to the Fermi-LAT instrument. In fact, dark matter annihilation into two Standard Model particles with a radiated photon, a process known as internal bremsstrahlung, can also give sharp spectral features in the ray spectrum close to the dark matter mass [70]. The photon can arise from the final state radiation (FSR) or virtual charged particle radiation/virtual IB (VIB). Thus, the IB photons will be the total contributions from both FSR and VIB.

It is well known that the annihilation cross section of the LSP neutralinos into a pair of light SM fermions is strongly suppressed by a factor  $m_f^2/m_{\tilde{\chi}_1^0}^2$  due to the helicity properties of a highly non-relativistic pair of Majorana neutralinos. However, such suppression can be evaded if the fermion final states contain an additional photon  $f\bar{f}\gamma$ , particularly when the photon is emitted from virtual sfermions with a mass close to the LSP neutralino. Therefore, the IB effects may explain the 133 GeV Fermi-LAT gamma ray line [71, 72], or may predict a higher energy (for example 200 GeV) gamma ray line in No-Scale  $\mathcal{F}$ - $SU(5)$ . Furthermore, the EW or strong gauge boson IBs have considerably larger rates due to the larger gauge coupling constants. Recently, a complete calculation of the leading EW corrections to the LSP neutralino annihilations for various final states [73] shows that such corrections may significantly enhance the annihilation rates. Although those processes do not generate the pronounced spectral features in gamma rays like the corresponding electromagnetic (EM) corrections, the integrated photon yield may be enhanced up to two orders of magnitude compared to the tree level results, which may also be probed by the ongoing Fermi Space Telescope experiment. As such, we have ample motivation to study those regions of the viable parameter space with small mass differences between the LSP neutralino and light stau.

Our mission here then is to augment the SUSY neutralino annihilation rates to enhance detection opportunity for a nearly pure bino LSP ( $> 99\%$  bino). Through near degeneracy amongst the lightest slepton and light bino masses, we can certainly increase the annihilation rate and boost IB effects to a dominant contribution, albeit with downward pressure on the bino relic den-

sity. For a SUSY bino, this requires a compressed  $\Delta M(\tilde{\chi}_1^0, \tilde{\tau}_1) \simeq 0 - 2$  GeV, with associated decays proceeding through an off-shell or on-shell tau accordingly. Compression of the light stau mass to  $\Delta M(\tilde{\chi}_1^0, \tilde{\tau}_1) \simeq 0 - 2$  GeV can be achieved in No-Scale  $\mathcal{F}$ - $SU(5)$  quite naturally via slight shifts of the low energy boundary condition  $\tan\beta$ . The resultant minor increase in  $\tan\beta$  does lead to marginally enhanced light stau mixing effects in the stau sector, slightly lowering the light stau mass. Satisfaction of the CDM relic density in a traditional thermal manner leads to an intrinsic escalation in the baseline value of this parameter, from  $\tan\beta \simeq 19.5$  to  $\tan\beta \simeq 25$  for a corresponding upward escalation in the gaugino mass from  $M_{1/2} \simeq 400$  to  $M_{1/2} \simeq 1500$  [33]. Because of this, the supplemental incrementation of  $\tan\beta$  required to squeeze the light stau mass and LSP to near degeneracy recedes with an inflating SUSY mass scale. The positive deviation in  $\tan\beta$ , with possibly small shifts in the gaugino mass  $M_{1/2}$  and flippon mass  $M_V$ , are all that are required to achieve the 0–2 GeV delta between the light stau mass and the LSP in the large unprobed region of the parameter space. In particular, no variation of the top quark mass  $m_t$  (within its experimental uncertainty) is necessary. As a result, the SUSY spectrum undergoes only a negligible transition, and thus the rich phenomenology (setting aside the relic density constraint, which must now be satisfied through non-thermal mechanisms) prevails wholly preserved. Indeed, the wedge of model space remains relatively static and persists in the form of Ref. [33], the lone exception being small shifts in the  $\tan\beta$  contours and indiscernible shifts in  $M_{1/2}$  and  $M_V$ .

From this perspective, the No-Scale  $\mathcal{F}$ - $SU(5)$  SUSY spectra corresponding to the wedge of viable model space provided in Ref. [33], duly suppressing the light stau mass, are potentially testable by the Fermi Space Telescope or a future gamma ray telescope; moreover, the two variations in determination of the light stau mass may be observationally distinguished. Crucially, experimental results from both the LHC and the LAT can be connected to the same SUSY spectrum, providing the type of cross-correlation testing which may play a significant role in substantiating any SUSY GUT model. In particular, probing of a specific  $(\tilde{\chi}_1^0, \tilde{t}_1, \tilde{g}, \tilde{q})$  point in the SUSY parameter space may potentially be achieved via dual experimental methodologies. This is possible since the No-Scale  $\mathcal{F}$ - $SU(5)$  SUSY spectrum exhibits the rather special attribute of leading order *en masse* proportionality to only  $M_{1/2}$ . Specifically, the internal physics of  $\mathcal{F}$ - $SU(5)$  are predominantly invariant under a numerical rescaling of only  $M_{1/2}$ . Consequently, each sparticle within the SUSY spectrum can be multiplicatively adjusted by an identical trivial rescaling of only  $M_{1/2}$ , though the linear slope relationship between  $M_{1/2}$  and each sparticle can vary. From a practical point of view, this property of No-Scale  $\mathcal{F}$ - $SU(5)$  permits the SUSY spectrum to be approximately determined from only a given value of  $M_{1/2}$ , or alternatively, from only a given

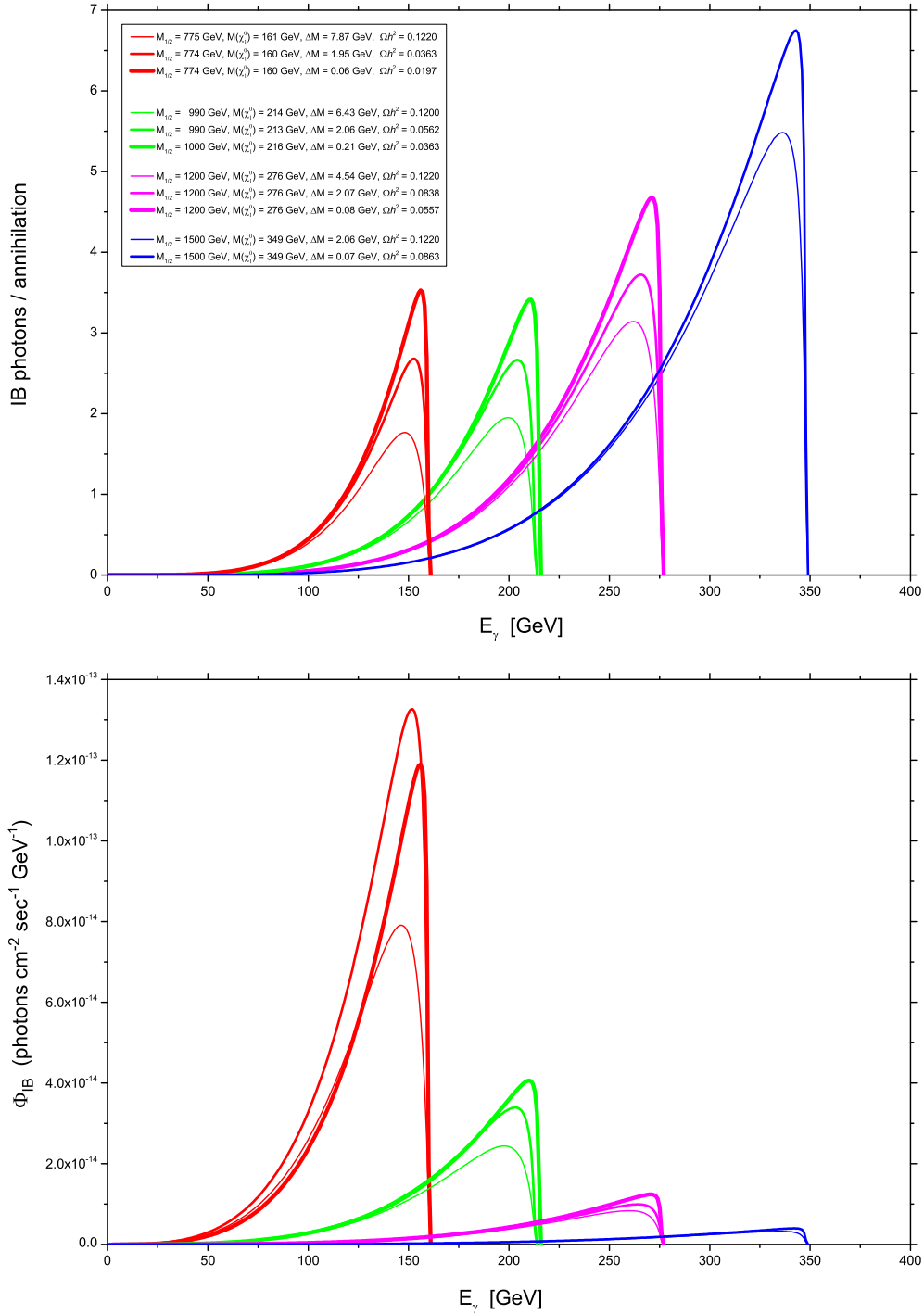


FIG. 1: No-Scale  $\mathcal{F}$ - $SU(5)$  Electromagnetic IB spectrum, given in terms of photons per annihilation (top frame) and differential flux (bottom frame), as a function of energy. All curves represent the benchmarks given in Tables I-II. The thin curves (lower) in both frames satisfy the Planck satellite relic density measurements  $\Omega h^2 = 0.1199 \pm 0.0027$ , while the thicker curves (middle) possess  $\Delta M(\tilde{\chi}_1^0, \tilde{\tau}_1) \simeq 2 \text{ GeV}$  and the thickest curves (upper) have  $\Delta M(\tilde{\chi}_1^0, \tilde{\tau}_1) \simeq 0 \text{ GeV}$ . Inclusion of the EW IB photon flux enhancement is reserved for a future work. The  $M_{1/2} = 774 - 775 \text{ GeV}$  benchmarks are consistent with the previously observed 133 GeV monochromatic gamma ray line. The  $\Delta M$  value given in the plot legend refers to the lightest neutralino and light stau mass difference. All IB photon counts and fluxes are calculated with **DarkSUSY 5.1.1**. For the local dark matter relic density, we use the value  $\rho_0 = 0.3 \text{ GeV/cm}^3$ . All differential fluxes are in units of photons  $\text{cm}^{-2} \text{sec}^{-1} \text{GeV}^{-1}$  and all masses are in GeV. The  $\Omega h^2$  shown in the plot legend is the thermal neutralino relic density calculated with **MicrOMEGAs 2.4**. For those benchmarks with  $\Omega h^2 < 0.1199 \pm 0.0027$ , the Planck satellite measured relic density can be generated via non-thermal mechanisms. The curves demonstrate that compression of the lightest bino neutralino and light stau mass delta does in fact enhance the EM IB effects.

TABLE I: Ten No-Scale  $\mathcal{F}$ - $SU(5)$  benchmarks, with points that can satisfy the Planck satellite relic density measurements, points with  $\Delta M(\tilde{\chi}_1^0, \tilde{\tau}_1) \simeq 2$  GeV, and points imposing degeneracy,  $\Delta M(\tilde{\chi}_1^0, \tilde{\tau}_1) \simeq 0$  GeV, between the light stau and LSP mass in order to increase the annihilation rate and raise the IB contributions. Given are the gaugino mass  $M_{1/2}$ , flippon mass  $M_V$ ,  $\tan\beta$ , top quark mass  $m_t$ , relic density  $\Omega h^2$ , EM  $f\bar{f}$ ,  $\gamma\gamma$ , and  $\gamma Z$  annihilation cross-sections, SUSY masses, and light Higgs boson mass  $m_h$ . All benchmark LSP compositions are greater than 99% bino. The  $\Omega h^2$  shown is the thermal neutralino density calculated with **MicrOMEGAS 2.4**. For those benchmarks with  $\Omega h^2 < 0.1199 \pm 0.0027$ , the Planck satellite measured relic density can be generated via non-thermal mechanisms. The annihilation cross-sections given here are the average between the **MicrOMEGAS 2.4** and **DarkSUSY 5.1.1** calculations. The total  $\langle\sigma v\rangle_{f\bar{f}}$  annihilation cross-section is composed of  $\langle\sigma v\rangle_{f\bar{f}} = \langle\sigma v\rangle_{\tau+\tau^-} + \langle\sigma v\rangle_{t\bar{t}} + \langle\sigma v\rangle_{b\bar{b}}$ . The  $\Delta M$  value refers to the lightest bino neutralino and light stau mass difference. The light Higgs boson mass includes both the tree level+1-loop+2-loop+3-loop+4-loop and flippon contributions. All masses are in GeV and all cross-sections in  $\text{cm}^3/\text{sec}$ .

$M_{1/2}$	$M_V$	$\tan\beta$	$m_t$	$\Omega h^2$	$\langle\sigma v\rangle_{f\bar{f}}$	$\langle\sigma v\rangle_{\gamma\gamma}$	$\langle\sigma v\rangle_{\gamma Z}$	$m_{\tilde{\chi}_1^0}$	$m_{\tilde{\tau}_1}$	$\Delta M$	$m_{\tilde{\chi}_2^0, \tilde{\chi}_1^\pm}$	$m_{\tilde{t}_1}$	$m_{\tilde{g}}$	$m_{\tilde{u}_R}$	$m_h$
775	4800	22.5	174.4	0.122	$68.5 \times 10^{-30}$	$2.61 \times 10^{-30}$	$0.98 \times 10^{-30}$	161	169	7.87	342	861	1047	1475	124.4
774	4821	23.0	174.4	0.036	$77.9 \times 10^{-30}$	$3.01 \times 10^{-30}$	$1.11 \times 10^{-30}$	160	162	1.95	341	860	1046	1473	124.4
774	4851	23.1	174.4	0.020	$81.1 \times 10^{-30}$	$3.19 \times 10^{-30}$	$1.16 \times 10^{-30}$	160	160	0.06	341	860	1046	1473	124.4
990	8044	23.3	174.4	0.120	$45.6 \times 10^{-30}$	$1.73 \times 10^{-30}$	$0.69 \times 10^{-30}$	214	220	6.43	449	1104	1328	1824	125.1
990	8070	23.6	174.4	0.056	$47.6 \times 10^{-30}$	$1.88 \times 10^{-30}$	$0.76 \times 10^{-30}$	213	216	2.06	449	1104	1328	1824	125.1
1000	8083	23.7	174.4	0.036	$46.7 \times 10^{-30}$	$1.93 \times 10^{-30}$	$0.77 \times 10^{-30}$	216	216	0.21	454	1116	1341	1841	125.2
1200	30, 830	24.3	173.3	0.122	$20.5 \times 10^{-30}$	$1.26 \times 10^{-30}$	$0.51 \times 10^{-30}$	276	281	4.54	572	1335	1633	2102	124.1
1200	30, 830	24.4	173.3	0.084	$20.8 \times 10^{-30}$	$1.31 \times 10^{-30}$	$0.53 \times 10^{-30}$	276	279	2.07	572	1335	1634	2102	124.1
1200	30, 830	24.5	173.3	0.056	$21.1 \times 10^{-30}$	$1.36 \times 10^{-30}$	$0.55 \times 10^{-30}$	276	277	0.08	572	1335	1634	2102	124.1
1500	27, 636	24.7	174.4	0.122	$8.88 \times 10^{-30}$	$0.85 \times 10^{-30}$	$0.35 \times 10^{-30}$	349	351	2.06	717	1661	2009	2602	126.3
1500	27, 636	24.8	174.4	0.086	$8.93 \times 10^{-30}$	$0.88 \times 10^{-30}$	$0.36 \times 10^{-30}$	349	349	0.07	717	1661	2009	2602	126.3

TABLE II: The ten No-Scale  $\mathcal{F}$ - $SU(5)$  benchmarks of Table I, with the IB photon flux  $\Phi_{IB}$  from  $\tilde{\chi}\tilde{\chi} \rightarrow f\bar{f}\gamma$  events, the photon flux  $\Phi_{\gamma\gamma}$  from  $\tilde{\chi}\tilde{\chi} \rightarrow \gamma\gamma$  events, and the photon flux  $\Phi_{\gamma Z}$  from  $\tilde{\chi}\tilde{\chi} \rightarrow \gamma Z$  events. The IB flux has been integrated across energy relative to the differential flux plotted in Figure 1. All fluxes are also integrated over the solid line-of-sight angle from the center of our galaxy, taking a detector acceptance of 2.5 steradians corresponding to the LAT instrument's 20% sky field of view, and are in units of photons  $\text{cm}^{-2} \text{sec}^{-1}$ . All fluxes are calculated with **DarkSUSY 5.1.1**. The  $\gamma\gamma$  flux includes the factor of 2 for the two photons. For the local dark matter relic density, we use the value  $\rho_0 = 0.3 \text{ GeV}/\text{cm}^3$ , with the spherically symmetric NFW halo profile. The column entry  $\Phi_{IB}/\Phi_{\gamma\gamma}$  is indicative of the increase in the magnitude of the IB flux over the gamma pair flux, and the adjacent column  $\Phi_{\gamma\gamma}/\Phi_{\gamma Z}$  likewise compares the gamma pair flux to that of the photon plus Z-boson. The final two columns provide the gamma radiation energy in GeV at the IB spectrum peak and its relation to the LSP mass in GeV.

$M_{1/2}$	$M_V$	$\tan\beta$	$m_t$	$\Phi_{IB}$	$\Phi_{\gamma\gamma}$	$\Phi_{\gamma Z}$	$\Phi_{IB}/\Phi_{\gamma\gamma}$	$\Phi_{\gamma\gamma}/\Phi_{\gamma Z}$	IB Peak	$m_{\tilde{\chi}_1^0}$
775	4800	22.53	174.4	$3.9 \times 10^{-12}$	$4.9 \times 10^{-13}$	$5.5 \times 10^{-14}$	8.1	8.7	148	161
774	4821	22.95	174.4	$5.8 \times 10^{-12}$	$5.6 \times 10^{-13}$	$6.2 \times 10^{-14}$	10.3	9.0	153	160
774	4851	23.08	174.4	$4.6 \times 10^{-12}$	$4.0 \times 10^{-13}$	$4.4 \times 10^{-14}$	11.5	9.1	156	160
990	8044	23.34	174.4	$1.5 \times 10^{-12}$	$1.8 \times 10^{-13}$	$2.3 \times 10^{-14}$	8.4	8.0	200	214
990	8070	23.61	174.4	$1.9 \times 10^{-12}$	$2.0 \times 10^{-13}$	$2.4 \times 10^{-14}$	9.8	8.1	204	213
1000	8083	23.73	174.4	$2.1 \times 10^{-12}$	$2.0 \times 10^{-13}$	$2.4 \times 10^{-14}$	10.7	8.1	211	216
1200	30, 830	24.26	173.3	$6.5 \times 10^{-13}$	$7.9 \times 10^{-14}$	$1.0 \times 10^{-14}$	8.2	7.8	262	276
1200	30, 830	24.41	173.3	$7.3 \times 10^{-13}$	$8.2 \times 10^{-14}$	$1.1 \times 10^{-14}$	8.9	7.8	266	276
1200	30, 830	24.53	173.3	$8.1 \times 10^{-13}$	$8.5 \times 10^{-14}$	$1.1 \times 10^{-14}$	9.6	7.8	271	276
1500	27, 636	24.67	174.4	$3.0 \times 10^{-13}$	$3.4 \times 10^{-14}$	$4.3 \times 10^{-15}$	8.8	7.8	336	349
1500	27, 636	24.77	174.4	$3.3 \times 10^{-13}$	$3.5 \times 10^{-14}$	$4.4 \times 10^{-15}$	9.4	7.8	343	349

value of any other sparticle mass, exhibiting the pragmatic predictive elegance of the model.

The final ingredient of our strategy involves derivation of a suitable set of benchmarks for comparison to experiment. We present ten benchmarks in Table I, with gaugino mass  $M_{1/2}$ , flippon mass  $M_V$ ,  $\tan\beta$ , top quark mass  $m_t$ , relic density  $\Omega h^2$ , EM  $f\bar{f}$ ,  $\gamma\gamma$ , and  $\gamma Z$  annihilation cross-sections, SUSY masses, and light Higgs boson mass. All benchmark LSP compositions are greater than 99% bino. The points have been extracted from a broad numerical scan, utilizing `MicrOMEGAs 2.1` [74] to compute SUSY mass spectra and a proprietary modification of the `SuSpect 2.34` [75] codebase to run the flippon enhanced RGEs. To be consistent with previous No-Scale  $\mathcal{F}$ - $SU(5)$  parameter space analyses [18, 33], we show in Table I the thermal relic density as computed by the updated routines in `MicrOMEGAs 2.4` [76]. Serving as a secondary verification, we further compute the thermal relic density with `DarkSUSY 5.1.1` [77, 78], reading as input an SLHA [79, 80] mass file generated from the flippon enhanced RGEs in our proprietary version of the `SuSpect 2.34` [75] codebase, finding only a small variation in the respective relic density computations. The annihilation cross-sections  $\langle\sigma v\rangle_{f\bar{f}}$ ,  $\langle\sigma v\rangle_{\gamma\gamma}$ , and  $\langle\sigma v\rangle_{\gamma Z}$  are calculated with both `MicrOMEGAs 2.4` and `DarkSUSY 5.1.1`, where we show the average of the two calculations in Table I. The total  $\langle\sigma v\rangle_{f\bar{f}}$  annihilation cross-section includes the only three non-negligible contributions in No-Scale  $\mathcal{F}$ - $SU(5)$  for a nearly pure SUSY bino:  $\langle\sigma v\rangle_{f\bar{f}} = \langle\sigma v\rangle_{\tau^+\tau^-} + \langle\sigma v\rangle_{t\bar{t}} + \langle\sigma v\rangle_{b\bar{b}}$ . The  $\Delta M$  value in Table I refers specifically to the light neutralino and light stau mass difference, which we are compressing to increase the annihilation rate and IB effects. The light Higgs boson mass  $m_h$  in Table I includes both the tree level+1-loop+2-loop+3-loop+4-loop contributions and the additional vector-like flippon contribution [33].

Expected photon flux rates are listed in Table II for the annihilation channels  $\tilde{\chi}\tilde{\chi} \rightarrow f\bar{f}\gamma$ ,  $\tilde{\chi}\tilde{\chi} \rightarrow \gamma\gamma$ , and  $\tilde{\chi}\tilde{\chi} \rightarrow \gamma Z$ , for the same ten No-Scale  $\mathcal{F}$ - $SU(5)$  benchmarks of Table I. For the local dark matter relic density, we use the value  $\rho_0 = 0.3 \text{ GeV/cm}^3$ , adopting the spherically symmetric NFW dark matter halo profile. The square of the dark matter density is integrated along the line of sight for each orientation within an angular detector acceptance of 2.5 steradians (sr) about the galactic center. This value is selected in correspondence with the LAT instrument's field of view, which encompasses about 20% of the sky at any given moment. Results are not overly sensitive to this parameter, given a value sufficiently wide to encapsulate the region of primary density. Since the IB scenario represents a continuum of radiation frequencies, the differential fluxes plotted in the lower panel of Figure 1 are integrated across energy to yield consistent units of photon counts per square centimeter per second in Table II. All fluxes are computed with `DarkSUSY 5.1.1`. The  $\gamma\gamma$  flux includes the factor of 2 for the two photons. The ratio  $\Phi_{IB}/\Phi_{\gamma\gamma}$  in Table II

represents the magnitude of the integrated IB flux relative to the  $\gamma\gamma$  line flux, which provides an advantage of about 10 across the full model space. Likewise, the column  $\Phi_{\gamma\gamma}/\Phi_{\gamma Z}$  reports the ratio of monochromatic flux rates for a gamma pair relative to a gamma plus Z-boson, which similarly yields an advantage of one magnitude order across the model space.

It is evident from Figure 1 that compressing the light bino neutralino and light stau does indeed enhance the EM IB effects for the benchmarks of Table I. The curves in the top frame of Figure 1 depict the number of IB photons per annihilation resulting from annihilation into charged particles. The bottom frame illustrates the IB flux  $\Phi_{IB}$  energy spectrum for the same ten benchmarks. The thin curves (lower) in both frames represent a region of the No-Scale  $\mathcal{F}$ - $SU(5)$  model space where the thermal LSP relic density can satisfy the Planck satellite CDM measurements  $\Omega h^2 = 0.1199 \pm 0.0027$  [38]. The thicker curves (middle) in both frames possess an LSP and light stau mass difference of about 2 GeV, with the thickest curves (upper) having a degenerate LSP and light stau, with possibly a long-lived light stau in this degenerate scenario. All IB photon counts in Figure 1 are computed with `DarkSUSY 5.1.1`, as are the IB fluxes. Clearly, the EM IB photon count, and hence the flux, increases for smaller  $\Delta M$ , an effect we presume will be enhanced when also including the EW contributions [73]. We leave the numerical results of the EW IB photon yield and additional flux for a future work [81]. At this juncture, we are content with a projection that the photon counts and fluxes in Figure 1 could be amplified via the additional EW IB contributions [73].

Our scale for the benchmarks in Tables I-II and Figure 1 begins at  $M_{1/2} = 775 \text{ GeV}$ , which is in the vicinity of the scale threshold that may be considered firmly excluded from the No-Scale  $\mathcal{F}$ - $SU(5)$  model space by the LHC SUSY search, as based upon a Monte Carlo event analysis [32]. We select sufficient points to provide thorough coverage of the entire viable model space. We direct attention to the region of the parameter space exemplified by the  $M_{1/2} = 774 - 775 \text{ GeV}$  benchmarks of Tables I-II as that consistent with an upper  $2\sigma$  limit on the WIMP mass that can explain the previously observed 133 GeV monochromatic gamma ray line. Comparing Figure 1 with Table II, it is apparent that compression of the  $\Delta M(\tilde{\chi}_1^0, \tilde{\tau}_1)$  mass gap substantially strengthens the IB signal in the narrowly peaked spectral range close to the LSP mass, whereas the advantage in integrated photon flux is less pronounced; this is relevant given higher experimental sensitivity to signals that more closely approximate a line spike.

## V. SUMMARY OF EXPERIMENTAL PROSPECTS

In this final section, we attempt to make a quantitative, if in some regards naïve, assessment of the experimen-



tal prospects of the various  $\mathcal{F}$ - $SU(5)$  model benchmarks previously described. The primary metric for assessment will be the integrated photon flux, *i.e.* the area under each differential flux curve displayed in the lower element of Figure 1, in units of photons  $\text{cm}^{-2} \text{sec}^{-1}$ , as reported in Table II. Since both background (following a power law with spectral index  $-2$ ) and the internal bremsstrahlung signal accrue in linear proportion with time, the  $S/\sqrt{B}$  signal to background discriminant may be expected to scale as the square root of time. Based upon four years of data collection in whole-sky survey mode (achieving a full  $4\pi$  steradian coverage once per two earth orbits), the Fermi collaboration has established sensitivity at five standard deviations to gamma flux rates above about  $3 - 4 \times 10^{-9} \text{ cm}^{-2} \text{ sec}^{-1}$  for line sources positioned at high galactic latitudes [82]; the sensitivity is diminished by about half an order of magnitude in the highly active galactic center. Taking an active Fermi mission lifetime of ten years, one sees that the data doubling advantage has already been largely depleted in the existing results, although the remaining multiple of 2.5 in integrated time may yet garner an improvement of around 1.6 deviations in sensitivity; in other words, any potential discovery apparent by the end of the Fermi mission should already be showing evidence above three standard deviations. Likewise, the expected end of mission line sensitivity may be projected at about  $2 \times 10^{-9} \text{ cm}^{-2} \text{ sec}^{-1}$ .

The root- $t$  scaling is actually a bit pessimistic for signals approximating a line width, and better sensitivity is possible. Additionally, the Fermi instrument has begun a transition toward more targeted observation of the galactic center for the remainder of its mission, which may garner an additional factor of about two in sensitivity, admitting however that baseline sensitivities are lower in this region. Likewise, substantial improvements in understanding of the detector and relevant analysis techniques are poised to reduce background contamination and improve overall instrument sensitivity [83]; we likewise assign a factor of about two to processing upgrades of this type, which are retroactive to already collected data. Holding backgrounds constant, a further reduction in the signal flux by a factor around  $3/5$  would still be capable of presenting strong evidence for a scale-localized excess. Together, then, we set a working threshold around  $3 \times 10^{-10} \text{ cm}^{-2} \text{ sec}^{-1}$  on any potentially visible gamma flux. Given continuum dispersion of the IB gamma signal, it is somewhat over optimistic to apply sensitivities extrapolated from line-signal searches, and this deficiency becomes more pronounced at higher mass scales with widening and flattening of the signal profile, as is visible in Figure 1. Nevertheless, it is important to recognize that any IB gamma signal may be compounded with line signals from loop order neutralino annihilation to gamma pairs and/or gamma Z, in the same basic spectral range, although potentially substantially suppressed, as indicated in Table II. Without an appreciable boost factor  $\mathcal{O}(50-100)$  in the computed annihilation rate, the  $\mathcal{F}$ - $SU(5)$  IB gamma flux, while more favorable for de-

tection than the flux associated with mono-energetic line sources, may remain obscured by background processes to the LAT instrument. However, if there is any validity to the existing 130 GeV signal, then it becomes quite likely that some undiagnosed boost factor is actually in play. Plausible sources of this upward shift in the flux include underestimation of the local dark matter density (or corrections to the assumption of a smooth profile distribution), and internal bremsstrahlung contributions from EW or strong gauge bosons.

As a closing note, we draw attention to the increase in the thermally produced bino relic density in Table I for those points with  $\Delta M(\tilde{\chi}_1^0, \tilde{\tau}_1) \simeq 0 - 2 \text{ GeV}$ , as the gaugino mass  $M_{1/2}$  is lifted; this is due primarily to the incrementally larger LSP mass, and a corresponding slow increase in the value of  $\tan\beta$ , which tracks the elevation in  $M_{1/2}$ , automatically enhancing the light stau mixing for larger SUSY mass scales. Interestingly, the viable No-Scale  $\mathcal{F}$ - $SU(5)$  parameter space terminates near  $M_{1/2} \sim 1500 \text{ GeV}$ , with a nearly degenerate light stau and LSP, while concurrently maintaining the Planck observed relic density. Furthermore, if we consider an off-shell tau, the parameter space can be extended up to  $M_{1/2} \sim 1700 \text{ GeV}$  before incurring a charged light stau as the LSP. In this uppermost region of the model space, no alternate measures, such as non-thermally produced WIMPS, need be invoked to generate the correct relic density. This very large  $M_{1/2} \sim 1500 \text{ GeV}$  region may be probed by future gamma ray probe experiments, and any possible gamma ray line signals could be directly correlated to LHC results, where, given the strong light stau and LSP neutralino mass degeneracy in this portion of the model, one may make an additional intriguing prediction for LHC phenomenology: in light stau production, the tau and LSP neutralino missing momentum signal will be collinear.

## VI. CONCLUSIONS

We presented here a methodology for testing No-Scale Supergravity with the FERMI satellite's Large Area Telescope, and similar future gamma ray telescopes. For our testing vehicle, we chose the supersymmetric grand unified model No-Scale Flipped  $SU(5)$  with extra vector-like flippon multiplets derived from F-Theory, dubbed  $\mathcal{F}$ - $SU(5)$ . Building upon ample extant phenomenological motivation for No-Scale  $\mathcal{F}$ - $SU(5)$ , we discussed the potentially significant empirical support recently provided to cosmological models of inflation based upon No-Scale Supergravity by intrinsic Starobinsky-like conformance with the Planck measurements, for a suitable choice of superpotential parameters. Given this impetus, we discussed how compressing the light stau and LSP mass difference can increase the internal bremsstrahlung effects and thus enhance the photon count from annihilation to elevate detection probabilities, albeit with a reduced bino relic density. We additionally explained how the Planck

satellite observed relic density can nevertheless be generated through a non-thermal mechanism. For concrete examples, we gave several benchmark points with light stau and LSP mass differences of 0–2 GeV, achieved by slight upward shifts in the low energy boundary condition  $\tan\beta$ , in conjunction with negligible variations in the gaugino mass  $M_{1/2}$  and flippon mass  $M_V$ ; these modifications leave the SUSY spectrum, aside from the light stau mass, unchanged, preserving the rich phenomenology (modulo appeal to non-thermal mechanisms of relic density generation) that is currently being probed by the LHC and several other Beyond the Standard Model (BSM) experiments. While the IB mechanism emerges as a more favorable context for observing a gamma ray signal generated consistently with the  $\mathcal{F}$ - $SU(5)$  model than

monochromatic sources, a clear signal in the present generation instrument still requires a boost of order  $\mathcal{O}(50\text{--}100)$  in the expected rate of flux.

### Acknowledgments

This research was supported in part by the DOE grant DE-FG03-95-Er-40917 (DVN) and by the Natural Science Foundation of China under grant numbers 10821504, 11075194, 11135003, and 11275246 (TL). We also thank Sam Houston State University for providing high performance computing resources.

- 
- [1] H. Goldberg, “Constraint on the photino mass from cosmology,” *Phys. Rev. Lett.* **50**, 1419 (1983).
- [2] J. R. Ellis, J. S. Hagelin, D. V. Nanopoulos, K. A. Olive, and M. Srednicki, “Supersymmetric relics from the big bang,” *Nucl. Phys.* **B238**, 453 (1984).
- [3] E. Aprile et al. (XENON100 Collaboration), “Dark Matter Results from 225 Live Days of XENON100 Data,” *Phys.Rev.Lett.* **109**, 181301 (2012), 1207.5988.
- [4] R. Agnese et al. (CDMS Collaboration), “Dark Matter Search Results Using the Silicon Detectors of CDMS II,” *Phys.Rev.Lett.* (2013), 1304.4279.
- [5] D. Akerib et al. (LUX Collaboration), “First results from the LUX dark matter experiment at the Sanford Underground Research Facility,” (2013), 1310.8214.
- [6] W. Atwood et al. (LAT Collaboration), “The Large Area Telescope on the Fermi Gamma-ray Space Telescope Mission,” *Astrophys.J.* **697**, 1071 (2009), 0902.1089.
- [7] T. Bringmann, X. Huang, A. Ibarra, S. Vogl, and C. Weniger, “Fermi LAT Search for Internal Bremsstrahlung Signatures from Dark Matter Annihilation,” (2012), 1203.1312.
- [8] C. Weniger, “A Tentative Gamma-Ray Line from Dark Matter Annihilation at the Fermi Large Area Telescope,” (2012), 1204.2797.
- [9] 1235384, “Search for Gamma-ray Spectral Lines with the Fermi Large Area Telescope and Dark Matter Implications,” (2013), 1305.5597.
- [10] T. Cohen, M. Lisanti, T. R. Slatyer, and J. G. Wacker, “Illuminating the 130 GeV Gamma Line with Continuum Photons,” *JHEP* **1210**, 134 (2012), 1207.0800.
- [11] T. Li, J. A. Maxin, D. V. Nanopoulos, and J. W. Walker, “A 125.5 GeV Higgs Boson in  $\mathcal{F}$ - $SU(5)$ : Imminently Observable Proton Decay, A 130 GeV Gamma-ray Line, and SUSY Multijets and Light Stops at the LHC8,” *Eur.Phys.J.* **C72**, 2246 (2012), 1208.1999.
- [12] T. Li, J. A. Maxin, D. V. Nanopoulos, and J. W. Walker, “The Golden Point of No-Scale and No-Parameter  $\mathcal{F}$ - $SU(5)$ ,” *Phys. Rev.* **D83**, 056015 (2011), 1007.5100.
- [13] T. Li, J. A. Maxin, D. V. Nanopoulos, and J. W. Walker, “The Golden Strip of Correlated Top Quark, Gaugino, and Vectorlike Mass In No-Scale, No-Parameter  $\mathcal{F}$ - $SU(5)$ ,” *Phys. Lett.* **B699**, 164 (2011), 1009.2981.
- [14] T. Li, J. A. Maxin, D. V. Nanopoulos, and J. W. Walker, “Super No-Scale  $\mathcal{F}$ - $SU(5)$ : Resolving the Gauge Hierarchy Problem by Dynamic Determination of  $M_{1/2}$  and  $\tan\beta$ ,” *Phys. Lett. B* **703**, 469 (2011), 1010.4550.
- [15] T. Li, J. A. Maxin, D. V. Nanopoulos, and J. W. Walker, “Blueprints of the No-Scale Multiverse at the LHC,” *Phys. Rev.* **D84**, 056016 (2011), 1101.2197.
- [16] T. Li, J. A. Maxin, D. V. Nanopoulos, and J. W. Walker, “Ultra High Jet Signals from Stringy No-Scale Supergravity,” (2011), 1103.2362.
- [17] T. Li, J. A. Maxin, D. V. Nanopoulos, and J. W. Walker, “The Ultrahigh jet multiplicity signal of stringy no-scale  $\mathcal{F}$ - $SU(5)$  at the  $\sqrt{s} = 7$  TeV LHC,” *Phys.Rev.* **D84**, 076003 (2011), 1103.4160.
- [18] T. Li, J. A. Maxin, D. V. Nanopoulos, and J. W. Walker, “The Unification of Dynamical Determination and Bare Minimal Phenomenological Constraints in No-Scale  $\mathcal{F}$ - $SU(5)$ ,” *Phys.Rev.* **D85**, 056007 (2012), 1105.3988.
- [19] T. Li, J. A. Maxin, D. V. Nanopoulos, and J. W. Walker, “The Race for Supersymmetric Dark Matter at XENON100 and the LHC: Stringy Correlations from No-Scale  $\mathcal{F}$ - $SU(5)$ ,” *JHEP* **1212**, 017 (2012), 1106.1165.
- [20] T. Li, J. A. Maxin, D. V. Nanopoulos, and J. W. Walker, “A Two-Tiered Correlation of Dark Matter with Missing Transverse Energy: Reconstructing the Lightest Supersymmetric Particle Mass at the LHC,” *JHEP* **02**, 129 (2012), 1107.2375.
- [21] T. Li, J. A. Maxin, D. V. Nanopoulos, and J. W. Walker, “Prospects for Discovery of Supersymmetric No-Scale  $\mathcal{F}$ - $SU(5)$  at The Once and Future LHC,” *Nucl.Phys.* **B859**, 96 (2012), 1107.3825.
- [22] T. Li, J. A. Maxin, D. V. Nanopoulos, and J. W. Walker, “Has SUSY Gone Undetected in 9-jet Events? A Ten-Fold Enhancement in the LHC Signal Efficiency,” (2011), 1108.5169.
- [23] T. Li, J. A. Maxin, D. V. Nanopoulos, and J. W. Walker, “The  $\mathcal{F}$ -Landscape: Dynamically Determining the Multiverse,” *Inter.Jour.Mod.Phys.* **A27**, 1250121 (2012), 1111.0236.
- [24] T. Li, J. A. Maxin, D. V. Nanopoulos, and J. W. Walker, “Profumo di SUSY: Suggestive Correlations in the ATLAS and CMS High Jet Multiplicity Data,” (2011), 1111.4204.
- [25] T. Li, J. A. Maxin, D. V. Nanopoulos, and J. W. Walker,

- “A Higgs Mass Shift to 125 GeV and A Multi-Jet Supersymmetry Signal: Miracle of the Flippons at the  $\sqrt{s} = 7$  TeV LHC,” *Phys.Lett.* **B710**, 207 (2012), 1112.3024.
- [26] T. Li, J. A. Maxin, D. V. Nanopoulos, and J. W. Walker, “A Multi-Axis Best Fit to the Collider Supersymmetry Search: The Aroma of Stops and Gluinos at the  $\sqrt{s} = 7$  TeV LHC,” (2012), 1203.1918.
- [27] T. Li, J. A. Maxin, D. V. Nanopoulos, and J. W. Walker, “Chanel  $N^{\circ}5(\text{fb}^{-1})$ : The Sweet Fragrance of SUSY,” (2012), 1205.3052.
- [28] T. Li, J. A. Maxin, D. V. Nanopoulos, and J. W. Walker, “Non-trivial Supersymmetry Correlations between ATLAS and CMS Observations,” (2012), 1206.0293.
- [29] T. Li, J. A. Maxin, D. V. Nanopoulos, and J. W. Walker, “Correlating LHCb  $B_s^0 \rightarrow \mu^+\mu^-$  Results with the ATLAS-CMS Multijet Supersymmetry Search,” *Europhys.Lett.* **100**, 21001 (2012), 1206.2633.
- [30] T. Li, J. A. Maxin, D. V. Nanopoulos, and J. W. Walker, “Testing No-Scale  $\mathcal{F}-SU(5)$ : A 125 GeV Higgs Boson and SUSY at the 8 TeV LHC,” *Phys.Lett.* **B718**, 70 (2012), 1207.1051.
- [31] T. Li, J. A. Maxin, D. V. Nanopoulos, and J. W. Walker, “Primordial Synthesis:  $\mathcal{F}-SU(5)$  SUSY Multijets, 145-150 GeV LSP, Proton & Rare Decays, 125 GeV Higgs Boson, & WMAP7,” (2012), 1210.3011.
- [32] T. Li, J. A. Maxin, D. V. Nanopoulos, and J. W. Walker, “Correlated Event Excesses in LHC SUSY Searches at 7 & 8 TeV: New Physics or Conspiring Noise?,” *Eur.Phys.J.* **C73**, 2556 (2013), 1302.6579.
- [33] T. Li, J. A. Maxin, D. V. Nanopoulos, and J. W. Walker, “No-Scale  $\mathcal{F}-SU(5)$  in the Light of LHC, Planck and XENON,” *Jour.Phys.* **G40**, 115002 (2013), 1305.1846.
- [34] T. Li, J. A. Maxin, D. V. Nanopoulos, and J. W. Walker, “Constricted SUSY from No-Scale  $\mathcal{F}-SU(5)$ : A “Blind Spot” for LHC Top Quark Reconstruction?,” *EPL* **104**, 31001 (2013), 1306.4931.
- [35] “Search for strong production of supersymmetric particles in final states with missing transverse momentum and at least three b-jets using 20.1  $\text{fb}^{-1}$  of pp collisions at  $\sqrt{s} = 8$  TeV with the ATLAS Detector,” (2013), ATLAS-CONF-2013-061, URL <http://cdsweb.cern.ch/>.
- [36] L. Bergstrom, T. Bringmann, I. Cholis, D. Hooper, and C. Weniger, “New limits on dark matter annihilation from AMS cosmic ray positron data,” *Phys.Rev.Lett.* (2013), 1306.3983.
- [37] A. Egorov and E. Pierpaoli, “Constraints on dark matter annihilation by radio observations of M31,” *Physical Review D*, vol. 88, id. **023504** (2013), 1304.0517.
- [38] P. Ade et al. (Planck Collaboration), “Planck 2013 results. XVI. Cosmological parameters,” (2013), 1303.5076.
- [39] T. Moroi and L. Randall, “Wino cold dark matter from anomaly mediated SUSY breaking,” *Nucl.Phys.* **B570**, 455 (2000), hep-ph/9906527.
- [40] J. Ellis, D. V. Nanopoulos, and K. A. Olive, “No-Scale Supergravity Realization of the Starobinsky Model of Inflation,” *Phys.Rev.Lett.* **111**, 111301 (2013), 1305.1247.
- [41] J. Ellis, D. V. Nanopoulos, and K. A. Olive, “Starobinsky-like Inflationary Models as Avatars of No-Scale Supergravity,” *JCAP* **1310**, 009 (2013), 1307.3537.
- [42] J. Ellis, D. V. Nanopoulos, and K. A. Olive, “A No-Scale Framework for Sub-Planckian Physics,” (2013), 1310.4770.
- [43] A. A. Starobinsky, “A New Type of Isotropic Cosmological Models Without Singularity,” *Phys.Lett.* **B91**, 99 (1980).
- [44] V. F. Mukhanov and G. Chibisov, “Quantum Fluctuation and Nonsingular Universe. (In Russian),” *JETP Lett.* **33**, 532 (1981).
- [45] A. Starobinsky, “The Perturbation Spectrum Evolving from a Nonsingular Initially De-Sitter Cosmology and the Microwave Background Anisotropy,” *Sov.Astron.Lett.* **9**, 302 (1983).
- [46] E. Cremmer, S. Ferrara, C. Kounnas, and D. V. Nanopoulos, “Naturally Vanishing Cosmological Constant in  $N = 1$  Supergravity,” *Phys. Lett.* **B133**, 61 (1983).
- [47] J. R. Ellis, C. Kounnas, and D. V. Nanopoulos, “No Scale Supersymmetric Guts,” *Nucl. Phys.* **B247**, 373 (1984).
- [48] S. Ferrara, C. Kounnas, and F. Zwirner, “Mass formulae and natural hierarchy in string effective supergravities,” *Nucl. Phys.* **B429**, 589 (1994), hep-th/9405188.
- [49] E. Witten, “Dimensional Reduction of Superstring Models,” *Phys. Lett.* **B155**, 151 (1985).
- [50] T.-j. Li, J. L. Lopez, and D. V. Nanopoulos, “Compactifications of M theory and their phenomenological consequences,” *Phys.Rev.* **D56**, 2602 (1997), hep-ph/9704247.
- [51] D. V. Nanopoulos, “F-enomenology,” (2002), hep-ph/0211128.
- [52] S. M. Barr, “A New Symmetry Breaking Pattern for  $SO(10)$  and Proton Decay,” *Phys. Lett.* **B112**, 219 (1982).
- [53] J. P. Derendinger, J. E. Kim, and D. V. Nanopoulos, “Anti- $SU(5)$ ,” *Phys. Lett.* **B139**, 170 (1984).
- [54] I. Antoniadis, J. R. Ellis, J. S. Hagelin, and D. V. Nanopoulos, “Supersymmetric Flipped  $SU(5)$  Revitalized,” *Phys. Lett.* **B194**, 231 (1987).
- [55] J. Jiang, T. Li, and D. V. Nanopoulos, “Testable Flipped  $SU(5) \times U(1)_X$  Models,” *Nucl. Phys.* **B772**, 49 (2007), hep-ph/0610054.
- [56] J. L. Lopez, D. V. Nanopoulos, and K.-j. Yuan, “The Search for a realistic flipped  $SU(5)$  string model,” *Nucl. Phys.* **B399**, 654 (1993), hep-th/9203025.
- [57] J. Jiang, T. Li, D. V. Nanopoulos, and D. Xie, “F- $SU(5)$ ,” *Phys. Lett.* **B677**, 322 (2009).
- [58] J. Jiang, T. Li, D. V. Nanopoulos, and D. Xie, “Flipped  $SU(5) \times U(1)_X$  Models from F-Theory,” *Nucl. Phys.* **B830**, 195 (2010), 0905.3394.
- [59] R. Harnik, D. T. Larson, H. Murayama, and M. Thormeier, “Probing the Planck scale with proton decay,” *Nucl.Phys.* **B706**, 372 (2005), hep-ph/0404260.
- [60] J. R. Ellis, D. V. Nanopoulos, and K. A. Olive, “Flipped heavy neutrinos: From the solar neutrino problem to baryogenesis,” *Phys.Lett.* **B300**, 121 (1993), hep-ph/9211325.
- [61] J. R. Ellis, J. L. Lopez, D. V. Nanopoulos, and K. A. Olive, “Flipped angles and phases: A Systematic study,” *Phys.Lett.* **B308**, 70 (1993), hep-ph/9303307.
- [62] “Combination of CDF and D0 Results on the Mass of the Top Quark using up to 5.6  $\text{fb}^{-1}$  of data (The CDF and D0 Collaboration),” (2010), 1007.3178.
- [63] “LEPSUSYWG, ALEPH, DELPHI, L3, OPAL experiments, note LEPSUSYWG/04-01.1 and 04-02.1,” (2011), URL <http://lepsusy.web.cern.ch/lepsusy/Welcme.html>.
- [64] J. R. Ellis, A. B. Lahanas, D. V. Nanopoulos, and K. Tamvakis, “No-Scale Supersymmetric Standard Model,” *Phys. Lett.* **B134**, 429 (1984).
- [65] J. R. Ellis, C. Kounnas, and D. V. Nanopoulos,

- “Phenomenological  $SU(1, 1)$  Supergravity,” Nucl. Phys. **B241**, 406 (1984).
- [66] A. B. Lahanas and D. V. Nanopoulos, “The Road to No Scale Supergravity,” Phys. Rept. **145**, 1 (1987).
- [67] P. Ade et al. (Planck Collaboration), “Planck 2013 results. XXII. Constraints on inflation,” (2013), 1303.5082.
- [68] K. S. Stelle, “Classical Gravity with Higher Derivatives,” Gen.Rel.Grav. **9**, 353 (1978).
- [69] B. Whitt, “Fourth Order Gravity as General Relativity Plus Matter,” Phys.Lett. **B145**, 176 (1984).
- [70] T. Bringmann, L. Bergstrom, and J. Edsjo, “New Gamma-Ray Contributions to Supersymmetric Dark Matter Annihilation,” JHEP **0801**, 049 (2008), 0710.3169.
- [71] T. Bringmann and C. Weniger, “Gamma Ray Signals from Dark Matter: Concepts, Status and Prospects,” Phys.Dark Univ. **1**, 194 (2012), 1208.5481.
- [72] B. Shakya, “A 130 GeV Gamma Ray Signal from Supersymmetry,” Phys.Dark Univ. **2**, 83 (2013), 1209.2427.
- [73] T. Bringmann and F. Calore, “Significant Enhancement of Neutralino Dark Matter Annihilation,” (2013), 1308.1089.
- [74] G. Belanger, F. Boudjema, A. Pukhov, and A. Semenov, “Dark matter direct detection rate in a generic model with micrOMEGAs2.1,” Comput. Phys. Commun. **180**, 747 (2009), 0803.2360.
- [75] A. Djouadi, J.-L. Kneur, and G. Moultaka, “SuSpect: A Fortran code for the supersymmetric and Higgs particle spectrum in the MSSM,” Comput. Phys. Commun. **176**, 426 (2007), hep-ph/0211331.
- [76] G. Belanger, F. Boudjema, P. Brun, A. Pukhov, S. Rosier-Lees, et al., “Indirect search for dark matter with micrOMEGAs2.4,” Comput.Phys.Commun. **182**, 842 (2011), 1004.1092.
- [77] P. Gondolo, J. Edsjo, P. Ullio, L. Bergstrom, M. Schelke, et al., “DarkSUSY: Computing supersymmetric dark matter properties numerically,” JCAP **0407**, 008 (2004), astro-ph/0406204.
- [78] P. Gondolo, J. Edsjo, P. Ullio, L. Bergstrom, M. Schelke, E. Baltz, T. Bringmann, and G. Duda, “DarkSUSY Homepage,” (2013), URL <http://www.darksusy.org>.
- [79] P. Z. Skands et al., “SUSY Les Houches Accord: Interfacing SUSY Spectrum Calculators, Decay Packages, and Event Generators,” JHEP **07**, 036 (2004), hep-ph/0311123.
- [80] B. Allanach, C. Balazs, G. Belanger, M. Bernhardt, F. Boudjema, et al., “SUSY Les Houches Accord 2,” Comput.Phys.Commun. **180**, 8 (2009), 0801.0045.
- [81] T. Li, J. A. Maxin, D. V. Nanopoulos, and J. W. Walker (2013), in Preparation.
- [82] F. S. S. Center, “LAT Sensitivity,” (2014), URL <http://fermi.gsfc.nasa.gov/ssc/data/analysis/documentation/>
- [83] W. Atwood et al. (Collaboration S. Zimmer Fermi-LAT), “Pass 8: Toward the Full Realization of the Fermi-LAT Scientific Potential,” (2013), 1303.3514.